

Photochemistry of the three carboxypyridines in water: a pH dependent reaction

Florence Rollet,^a Claire Richard,^{*a} Jean-François Pilichowski^a and Bettina Aboab^b

^a Laboratoire de Photochimie Moléculaire et Macromoléculaire, UMR n°6505 CNRS-Université Blaise Pascal, F-63177 Aubière Cedex, France

^b Laboratoire de Synthèse, Electrosynthèse, Etude de Systèmes à Intérêt Biologique, UMR n°6504 CNRS-Université Blaise Pascal, F-63177 Aubière Cedex, France

Received 2nd February 2004, Accepted 26th May 2004

First published as an Advance Article on the web 23rd July 2004

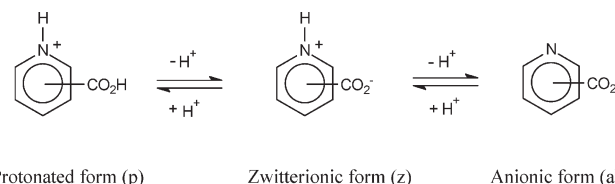
The photochemistry of *ortho*, *meta* and *para*-carboxypyridines ($pK_{a1} = 1.0\text{--}2.1$ and $pK_{a2} = 4.7\text{--}5.3$) in aqueous medium was studied by laser-flash photolysis and product studies. At $\text{pH} < pK_{a1}$, hydroxylated compounds are produced with low quantum yields. Within the pH range 4–7, *ortho* and *meta* isomers undergo dimerization together with decarboxylation with a quantum yield showing a very sharp maximum around pK_{a2} ($\phi_{\text{max}} = 0.09$ and 0.01, respectively) while the *para* isomer is photostable. End-of-pulse transients assigned to triplet states were detected by laser-flash photolysis at $\text{pH} < pK_{a1}$ and $\text{pH} > 4$. Additionally, the carboxypyridinyl radicals were detected as secondary intermediates at $\text{pH} < pK_{a1}$ and $4 < \text{pH} < 7$ and the OH-adduct radicals at $\text{pH} < pK_{a1}$. This is in favour of an electron transfer reaction between triplet and starting compound producing a charge transfer species. The radical anion would escape as carboxypyridinyl radical while the radical cation may add water at $\text{pH} < pK_{a1}$ yielding the OH-adduct radical or may undergo decarboxylation at $\text{pH} > 4$. The high quantum yield of phototransformation of the *ortho* isomer at $\text{pH} > 4$ is due to an easy decarboxylation process. A reaction scheme is proposed accounting for the dependences of ϕ on both the pH and the carboxypyridines concentration. This study points out the distinct pattern of reactivity of carboxypyridines depending on the ionisation state of starting compounds and isomeric substitution.

Introduction

Photochemistry of nitrogen heterocycles has received much attention owing to the importance of these compounds in chemistry and biochemistry, most of the reactions having been investigated in organic solvents. Pyridine and methylpyridines were found to undergo photoisomerisation and photosubstitution in organic solvents.¹ The intermediary formation of diradicals was suggested.^{2,3} Pyridines substituted by a SH group in an *ortho* or *para* position with respect to the N atom are mainly in the thione form. They were found to populate very efficiently their triplet state under irradiation in organic solvents. These triplets were proved to be capable of abstracting an electron from a donor or giving an electron to an acceptor.⁴ The triplet excited state of dicyanopyridines was detected too in acetonitrile.⁵ It was reported that these triplets are reduced by amines, *via* an electron transfer reaction, yielding pyridyl radical anion.⁶ The photochemistry of nitrogen heterocycles in aqueous solution has been much less investigated. In aqueous medium, pyridine was found to undergo ring opening with production of 5-amino-2,4-pentadienal ($\phi = 0.07$), this reaction being not affected by oxygen.⁷ The Dewar pyridine was proposed to be the key intermediate.⁸ The photochemistry of 2-chloropyrimidine was investigated due to its similarity with compounds of biological and medical interest. They were reported as undergoing a heterolytic scission of the C–Cl bond in the excited singlet state and a homolytic C–Cl scission in the triplet state that is efficiently populated upon irradiation at 266 nm in neutral medium.⁹

The photochemistry of 3-carboxypyridine, which is also a compound having biological significance, was investigated in water. It was reported to strongly depend on the pH.¹⁰ Indeed, 2-hydroxy-3-carboxypyridine is formed in very acidic media, while 2-(3-pyridyl)-pyridine-5-carboxylic acid is the main photoproduct in the pH range 4–6. In basic media, 3-carboxypyridine is almost photostable. Using the fact that oxygen inhibits the formation of 2-hydroxy-3-carboxypyridine, it was proposed that the reactivity in very acidic media arose from the triplet excited state.¹⁰ In a preliminary study, we could successfully detect the anionic triplet state of 3-carboxypyridine using nanosecond laser flash photolysis. Kinetic data suggested that it was involved in the bipyridine formation.¹¹

To get a better insight into the mechanism of the reaction of the three isomers, we undertook a detailed study varying pH. Depending on the pH, the carboxypyridines can exist in three forms. As seen from the pK_a values given in Table 1, the carboxyl group attached to the pyridinium nucleus is a very strong acid. Similarly the NH^+ group is about a ten times stronger acid than the corresponding methylpyridines. Neutral species exist predominantly in the zwitterionic form.^{12–14}



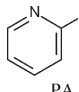
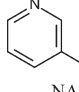
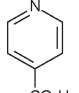
Results

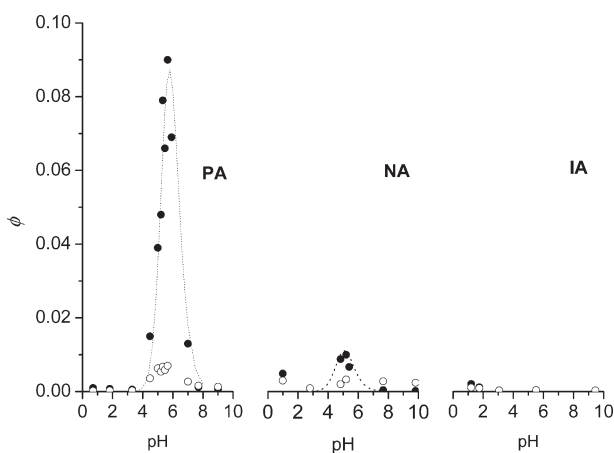
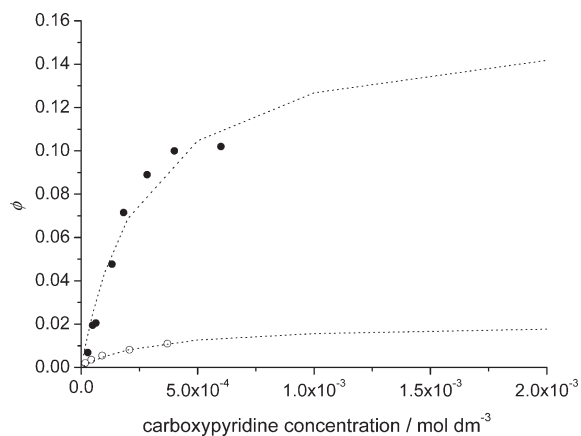
Steady-state irradiation

Quantum yields. The quantum yields of *ortho*-carboxypyridine (picolinic acid, PA), *meta*-carboxypyridine (nicotinic acid, NA), and *para*-carboxypyridine (isonicotinic acid, IA) phototransformation (ϕ) were measured in various conditions of pH. As shown in Fig. 1, they strongly depend on the pH and the substituent position. In the absence of oxygen, the quantum yields fell within the range 0.001–0.005 at $\text{pH} < 2$. The quantum yield of PA drastically increased from pH 4 to reach a maximum of 0.09 at pH 5.6 and decreased at higher pH to become negligible at $\text{pH} > 7$. A similar quantum yield evolution was observed for NA; however, the maximum was found to be lower, equal to 0.01 only. In contrast, the quantum yield of IA photolysis remained very low whatever the pH. Oxygen significantly reduced the quantum yields at $\text{pH} < 2$ (about twofold for NA and fivefold for PA) and within the pH range 4–7 (about threefold for NA at pH 5.2 and twelvefold for PA at pH 5.6).

The quantum yields of PA and NA phototransformation were also measured at substrate concentrations varying within the range $2 \times 10^{-5}\text{--}6 \times 10^{-4} \text{ mol dm}^{-3}$ at pH 5.6 and 5.2, respectively. In both cases, it increased with increasing concentration (Fig. 2, for dotted lines, see later).

Table 1 Equilibrium constants in aqueous solution of pyridine carboxylic acids¹² and absorption of anion and cation¹³

	pK_{a1}	pK_{a2}	$\lambda_{\max} (\epsilon_{\max})$ cation	$\lambda_{\max} (\epsilon_{\max})$ anion
 PA	1.04	5.29	265 (7600)	265 (4000)
 NA	2.11	4.77	262 (5000)	262 (3100)
 IA	1.86	4.84	272 (4600)	266 (2400)

**Fig. 1** Dependence of the quantum yields of PA, NA and IA (3×10^{-4} mol dm⁻³) photolysis on the pH. ●: deoxygenated medium; ○: oxygenated medium. The lines correspond to the curve fit (see text).**Fig. 2** Dependence of the quantum yield of NA and PA photolysis on NA and PA concentration. Deoxygenated medium. ●: PA, pH 5.6; ○: NA, pH 5.2. The lines correspond to the curve fit (see text).

Photoproducts. The irradiation of deoxygenated solutions of NA, PA and IA at pH 1 led to the formation of hydroxy derivatives. The yield was $\approx 40\%$ for the former two and 18% for the latter. Only 6-OH-PA and 2-OH-IA were formed from PA and IA, respectively. In contrast, 2-OH-NA (major) and 6-OH-NA (minor) were formed from NA. Moreover, the ¹H-NMR spectrum in D₂O of the crude irradiated mixture obtained from NA showed a new series of resonances in the olefinic (around 6 ppm) and aliphatic regions, that can be tentatively attributed to linear photoproducts derived from the pyridine ring opening.¹⁴ The general tautomerism phenomenon for most of 2-OH-pyridines that should be described as 2-pyridone in solution was observed.¹⁵ In the case of 2-OH-NA (3-carboxy-2-

pyridone) this fact is demonstrated by the presence of two peaks (at 164.6 and 165.1 ppm) in the carbonyl region of the ¹³C spectrum.

At $4 < \text{pH} < 7$, PA yielded 2-(3-pyridyl)-pyridine with a chemical yield of 28% as the only bipyridine (see experimental part). The irradiated solutions of NA were found to contain several photoproducts: 2-(3-pyridyl)-pyridine-5-carboxylic acid as the main photoproduct, 2-(3-pyridyl)-pyridine, dicarboxylated 2-(3-pyridyl)-pyridine, hydroxy derivatives and unidentified peaks that may correspond to carboxylated bipyridines on the basis of retention times and UV absorption spectrum. The chemical yield of 2-(3-pyridyl)-pyridine-5-carboxylic acid was found to be equal to 18% in solutions containing 7×10^{-4} mol dm⁻³ of NA.

Preliminary quantum semi-empirical SAM1¹⁶ calculations, carried out at the Unrestricted Hartree Fock (UHF) level using the AMPAC 7.0¹⁷ program, indicated that decarboxylation should occur. We therefore performed total organic carbon analyses in order to understand the fate of the CO₂ substituent. Indeed, photoextrusion of CO₂ should lead to a decrease of the total organic carbon while the loss of CO₂ as an organic molecule (formic acid for example) should not. NA (3.7×10^{-4} mol dm⁻³, pH 5.1) was irradiated in order to achieve a conversion extent of 40% corresponding to 10.5 mg dm⁻³ of converted organic carbon. TOC measurements revealed that solutions had lost 1 mg dm⁻³ of organic carbon. Similarly, PA (4.4×10^{-4} mol dm⁻³, pH 5.3) was irradiated in order to achieve a conversion extent of 29% corresponding to 8.9 mg dm⁻³ of converted organic carbon. We found that 0.9 mg dm⁻³ of organic carbon was evolved as CO₂.

Laser flash photolysis

pH < pK_{a1}. NA photolysis. The laser flash photolysis of NA (4×10^{-4} mol dm⁻³, pH 0.9) produced a long-lived and a short-lived transient species within the pulse (see insert A of Fig. 3). The spectrum of the short-lived transient was obtained by subtracting absorbances measured 1.6 μ s after the pulse from the end-of-pulse absorbances. It had a maximum of absorption at 435 nm. In deoxygenated medium, this transient decayed by apparent first order kinetics. The first order rate constant increased linearly with NA concentration. Linear regression gave $k = (3.7 \pm 0.3) \times 10^5 + (3.3 \pm 0.3) \times 10^9$ [NA] s⁻¹ (four experimental data, correlation coefficient = 0.99). In oxygen-saturated solution, the decay rate significantly increased. From the apparent first order rate constant ($6.2 \pm 0.6) \times 10^6$ s⁻¹, we deduced that the bimolecular rate constant of quenching by oxygen was equal to 3.4×10^9 mol⁻¹ dm³ s⁻¹. The 435 nm transient was formed in a monophotonic process as indicated by the linear dependence of the absorbance on the laser pulse energy, *P*. Using potassium peroxodisulfate as a chemical actinometer, we evaluated the product $\epsilon \times \phi$ of the extinction coefficient and quantum yield from the slope of the linear regression to be 120 ± 20 mol⁻¹ dm³ cm⁻¹ at 435 nm. The long-lived transient exhibited a maximum of absorption around 320 nm and a lifetime of about 500 μ s whatever the oxygen concentration.

Secondary transients with lifetimes of around 50 μ s could be detected in deoxygenated medium. From their build-up monitored at 290 nm (insert B of Fig. 3), it seems clear that these species are the daughters of the 435 nm transient. They were not detected in oxygen-saturated medium. Their absorption spectrum was obtained as follows. We first subtracted the absorbances measured 50 μ s after the pulse end from those measured 4 μ s after the pulse in deoxygenated medium, then, we corrected this spectrum for the contribution of the 320 nm long-lived end-of-pulse transient that was obtained by subtracting the absorbances measured 50 μ s after the pulse from those measured 4 μ s after in oxygen-saturated medium. As shown in Fig. 4, the secondary absorption showed two maxima at 285 and 415 nm and a shoulder around 325 nm. The products $\epsilon \times \phi$ of the secondary species were measured at 290 nm and 325 nm. In the former case, the contribution of the long-lived transient could be neglected and the $\epsilon \times \phi$ was obtained using the absorbances measured 2 μ s after the end of the pulse; we found 100 ± 20 mol⁻¹ dm³ cm⁻¹. In the latter, we made the difference between the absorbances measured 2 μ s after the end of the pulse in nitrogen-saturated

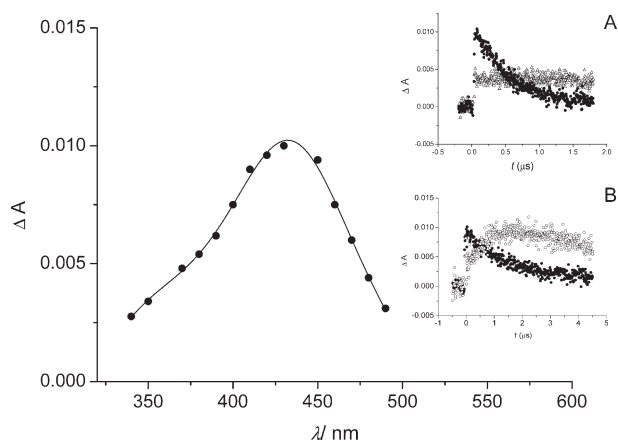


Fig. 3 Transient absorption spectrum from an aerated acidic (pH 0.9) solution of NA (4×10^{-4} mol dm $^{-3}$). Values obtained by subtracting absorbances measured 1.6 μ s after the pulse end from end-of-pulse absorbances. $\lambda_{\text{exc}} = 266$ nm. Insert A: time course absorbances at 435 nm (\bullet) and 320 nm (Δ) in oxygen-saturated medium. Insert B: time course absorbances at 435 nm (\bullet) and 290 nm (\circ) in deoxygenated medium.

solution and those measured 2 μ s in oxygen-saturated medium to correct for the contribution of the long-lived species. We obtained 40 ± 10 mol $^{-1}$ dm 3 cm $^{-1}$.

PA photolysis. The laser flash photolysis of acidic PA (1.4×10^{-4} mol dm $^{-3}$, pH 0.7) yielded the end-of-pulse transient absorption shown in Fig. 5. It exhibited two maxima at 306 and 350 nm. The transient spectrum measured 2 μ s after the pulse end slightly differed from the end-of-pulse spectrum suggesting the presence of secondary species. In oxygen-saturated medium, the end-of-pulse transient species showed a lifetime of 0.3 μ s; we deduced that the rate constant of quenching by oxygen was equal to 2.4×10^9 mol $^{-1}$ dm 3 s $^{-1}$. The product $\epsilon \times \phi$ at 305 nm was found to be 220 ± 50 and 130 ± 50 mol $^{-1}$ dm 3 cm $^{-1}$ at the pulse end and 3 μ s after the pulse end, respectively.

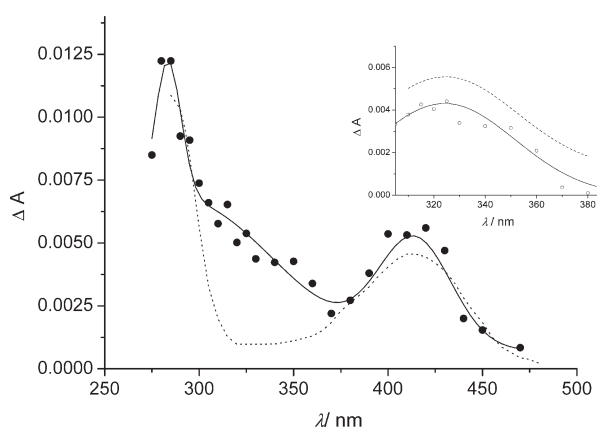


Fig. 4 Transient absorption spectra of secondary species obtained from deoxygenated acidic (pH 0.9) solution of NA (4×10^{-4} mol dm $^{-3}$) (\bullet , see text). $\lambda_{\text{exc}} = 266$ nm. Dotted line: transient spectrum of the 3-carboxypyridinyl radical.¹⁸ Insert: dash line: transient spectrum of OH-adduct radical from NA¹⁹ and \circ : difference between secondary transient spectrum and transient spectrum of 3-carboxypyridinyl radical.

IA photolysis. The photolysis of acidic IA (2.5×10^{-4} mol dm $^{-3}$, pH 0.96) yielded the pulse end transient spectrum given in Fig. 6. It exhibited two maxima at 310 and 380 nm. The lifetime of the species was found to be equal to 1.6 μ s in deoxygenated solution and 0.4 μ s in oxygen-saturated medium.

$\text{pH} \approx (\text{p}K_{a1} + \text{p}K_{a2})/2$. Only very weak absorbances were measured upon photolysis of the three isomers at pH 1.5 and 3.

$\text{pH} > 4$. **Photoionisation.** The irradiation of the three carboxypyridines at $\text{pH} \geq 6$ yielded the 725 nm characteristic absorption band of the solvated electrons at pulse end. The 725 nm

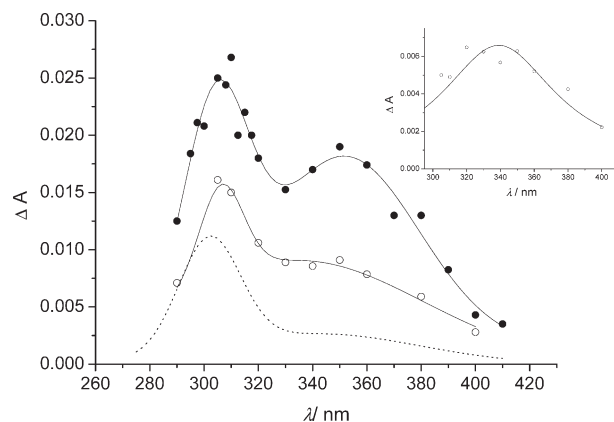


Fig. 5 Transient absorption spectrum from deoxygenated acidic (pH 0.7) solution of PA (1.4×10^{-4} mol dm $^{-3}$). \bullet Absorbances measured at pulse end; \circ absorbances measured 2 μ s after the pulse end; dotted line: transient spectrum of the 2-carboxypyridinyl radical.²⁰ $\lambda_{\text{exc}} = 266$ nm. Insert: difference between the transient spectrum measured 2 μ s after the pulse end and the transient spectrum of 2-carboxypyridinyl radical.

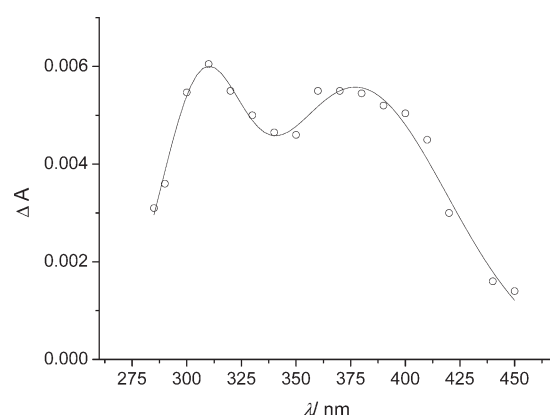


Fig. 6 Transient absorption spectrum from a deoxygenated acidic (pH 1) solution of IA (2.5×10^{-4} mol $^{-1}$ dm 3). \bullet values obtained at pulse end. $\lambda_{\text{exc}} = 266$ nm.

extrapolated absorbances typically increased with the laser pulse energy, P , in a quadratic way indicating that solvated electrons were produced in mixed mono and biphotonic processes (Fig. 7). In accordance, the plot of the ratio of the 725 nm extrapolated absorbances over P against P was linear (insert of Fig. 7). From the intercept, we could determine the products $\epsilon \times \phi$ corresponding to the monophotonic processes. We found 150, 250 and 300 mol $^{-1}$ dm 3 s $^{-1}$ for NA, PA and IA, respectively. Taking for the solvated electrons an extinction coefficient equal to 18500 mol $^{-1}$ dm 3 cm $^{-1}$ at 725 nm, we obtained $\phi_{\text{electron}} = 0.008, 0.0135$ and 0.016, respectively. At pH 4.1, NA did not produce measurable amounts of monophotonic solvated electrons.

Other transient species. In conditions under which photoionisation was negligible, the photolysis of deoxygenated solutions of NA (1.9×10^{-4} mol dm $^{-3}$, pH 8) yielded at end-of-pulse species exhibiting two maxima of absorption at 285 and 375 nm (Fig. 8) and decaying by apparent first order kinetics. The lifetime of this transient was about 4 μ s in deoxygenated medium while it reduced to 0.2 and 0.1 μ s in the presence of oxygen (1.3×10^{-3} mol $^{-1}$ dm 3) or methyl acrylate (5.0×10^{-3} mol $^{-1}$ dm 3), respectively. On this basis, it was previously assigned to the triplet excited state.¹¹

In the case of IA (2.3×10^{-4} mol $^{-1}$ dm 3), absorbances were rather weak and it was necessary to do measurements at high P values. To avoid secondary reactions induced by solvated electrons, we had to quench them by saturating the medium by N $_2$ O. Under these conditions, we observed a transient with maximum at 290 and 375 nm (Fig. 8). It decayed very fast in the absence of oxygen ($\tau < 0.1$ μ s).

The photolysis of PA (1.5×10^{-4} mol $^{-1}$ dm 3 , pH 5.6) produced an end-of-pulse absorption with a maximum at 290 nm and a shoulder around 340 nm (Fig. 9). 7 μ s after the pulse end, we measured a

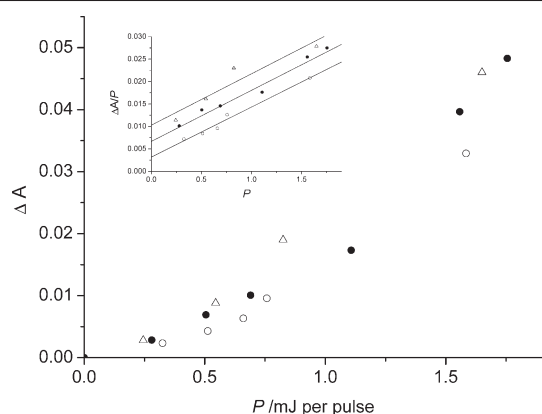


Fig. 7 Plot of pulse end absorbances measured at 725 nm vs. P , the laser energy pulse. \circ : NA at pH 6; \bullet : IA at pH 9; \triangle : PA at pH = 10. Inset: Plots of $\Delta A/P$ vs. P . Deoxygenated solutions; $\lambda_{\text{exc}} = 266$ nm.

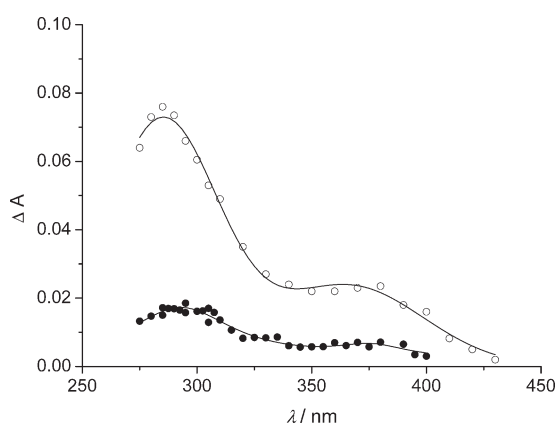


Fig. 8 Transient absorption spectra measured at the end of the pulse from deoxygenated solutions of NA (\circ , 1.9×10^{-4} M), and solutions of IA (\bullet , 2.3×10^{-4} M) saturated by N_2O . pH 5; $\lambda_{\text{exc}} = 266$ nm.

slightly different transient spectrum with, again, a strong band peaking at 290 nm and a weak band around 400 nm, build-up of which is shown in insert A of Fig. 9. The decay at 290 nm clearly indicated the presence of at least two species. Indeed, first order kinetics was observed within the first three μs following the pulse ($k = 1.25 \times 10^5 \text{ s}^{-1}$) while second order kinetics was observed at longer decay times (insert B of Fig. 9). In the presence of oxygen, the end-of-pulse transient readily disappeared with $k = 2.5 \times 10^6 \text{ s}^{-1}$ and the secondary species were not detected.

The influence of the initial substrate concentration on the disappearance of the end-of-pulse transient was investigated at $\text{pH} \approx \text{p}K_{\text{a}2}$ and in basic medium. In the case of NA and PA, the first order rate constant of decay increased linearly with increasing concentration

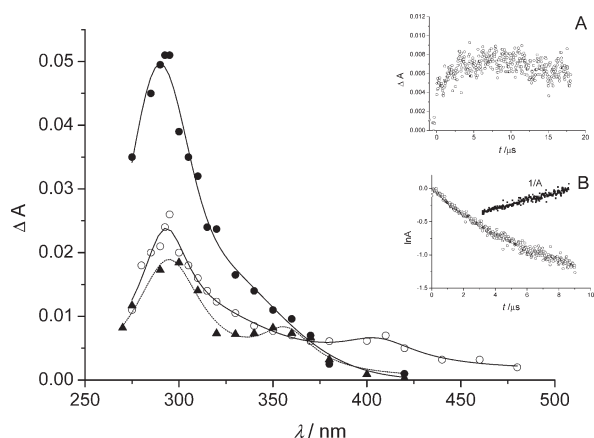


Fig. 9 Transient absorption spectra measured from PA ($1.5 \times 10^{-4} \text{ mol}^{-1} \text{ dm}^3$, pH 5.6): \bullet : at pulse end; \circ : 7 μs after the pulse end; \blacktriangle : transient spectrum of the 2-carboxypyridinyl radical.²⁰ Inset A: Time course absorbance at 400 nm. Inset B: Plots of $\ln A$ vs. t and $1/A$ vs. t , with A measured at 290 nm and pulse end.

(see Figs. 10A and B). Linear regression gave $k = (1.8 \pm 0.2) \times 10^5 + (4.9 \pm 0.4) \times 10^8 [\text{NA}] \text{ s}^{-1}$ at pH 10.9, $(2.3 \pm 0.1) \times 10^5 + (8.5 \pm 0.2) \times 10^8 [\text{NA}] \text{ s}^{-1}$ at pH 4.9, $(2.5 \pm 0.3) \times 10^5 + (6.7 \pm 0.7) \times 10^8 [\text{PA}] \text{ s}^{-1}$ at pH 5.1 and $(5.2 \pm 0.1) \times 10^4 + (1.8 \pm 0.5) \times 10^8 [\text{PA}] \text{ s}^{-1}$ at pH 10.1. The distinct slopes values at $\text{p}K_{\text{a}2}$ and in basic medium bring evidence that zwitterionic and anionic ground-state molecules react differently with the short-lived transient.

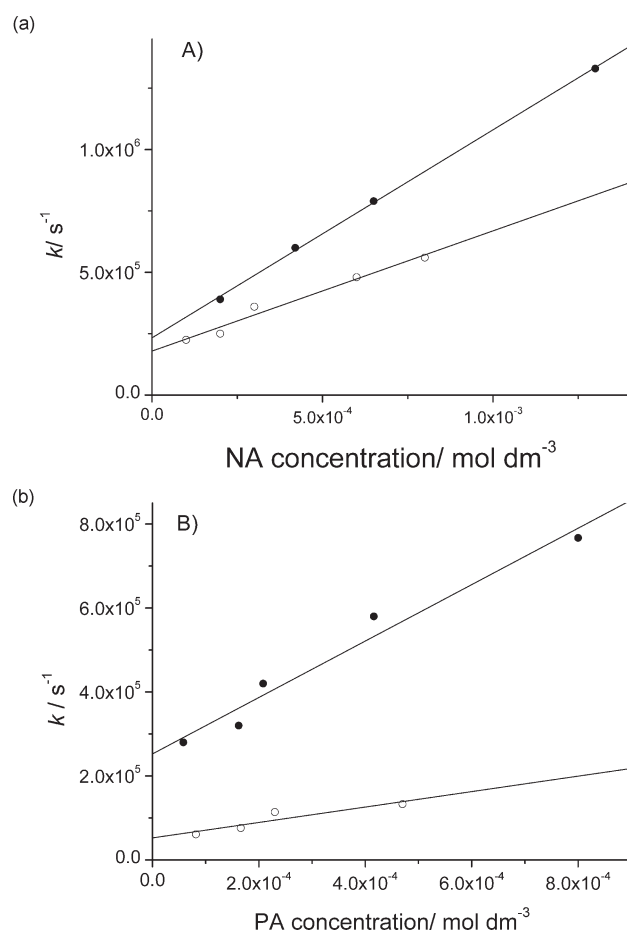


Fig. 10 Dependence of the triplet decay at 290 nm on NA (A) and PA (B) concentration. A) \bullet : pH = 4.9; \circ : pH = 10.9; B) \bullet : pH = 5.1; \circ : pH = 10.1.

Influence of the pH. We monitored the influence of pH on the product $\varepsilon \times \phi$ of the end-of-pulse transients and on their decay. As seen in Fig. 11, the product $\varepsilon \times \phi$ of the transient obtained from NA increased sharply with increasing pH from $200 \text{ mol}^{-1} \text{ dm}^3 \text{ cm}^{-1}$ at pH 2.9 to a plateau value of $3000 \text{ mol}^{-1} \text{ dm}^3 \text{ cm}^{-1}$ at pH 7. Data were well fitted by a sigmoidal curve centered at pH 4.9. A similar curve shape was obtained for the transient obtained from PA with a plateau value slightly lower than that of NA ($1700 \text{ mol}^{-1} \text{ dm}^3 \text{ cm}^{-1}$) and a center at pH 5.4. In each case, the center value was close to $\text{p}K_{\text{a}2}$.

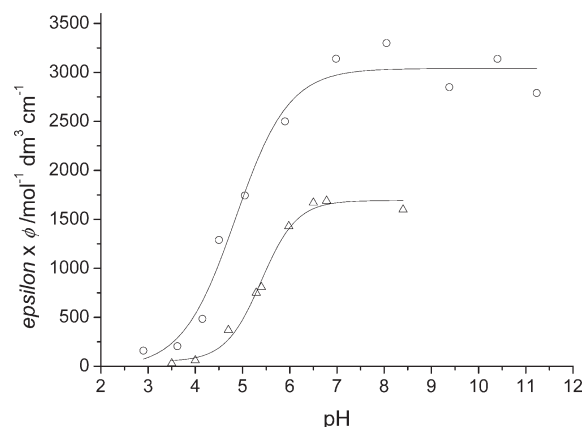


Fig. 11 Dependence of the $\varepsilon \times \phi$ product on the pH for NA (\circ) and PA (\triangle). $\lambda_{\text{exc}} = 266$ nm.

The decays of the end-of-pulse species arising from NA and PA were studied within the pH range 2.9–6.0, the species issued from IA decaying too fast to be studied. The apparent first order rate constants of decay were found to increase linearly with $[H^+]$. In the case of NA, the linear regression gave $k = (8.5 \pm 0.5) \times 10^5 + (4.6 \pm 0.4) \times 10^9 [H^+] s^{-1}$ (four experimental data, correlation coefficient = 0.99). The decay of the transient formed from PA could be only measured within the pH range 4.7–6. As for NA, we observed an increase of the decay rate with decreasing pH. Linear regression gave $k = (1.8 \pm 0.5) \times 10^5 + (1.7 \pm 0.5) \times 10^{10} [H^+] s^{-1}$ (three experimental data, correlation coefficient = 0.96).

Discussion

Assignment of transients

The laser-flash photolysis of the three isomers yielded two-band feature short-lived species at the pulse end. Some of their characteristics are summarized in Table 2. Based upon the scavenging effects of oxygen and methylacrylate, they can be assigned to the excited triplet states. Those observed at $pH > 4$ react with H^+ with rate constants close to the diffusion-controlled limit. Moreover, their yield of formation was found to increase with pH, and the curve to closely follow that of the ground state molecules second ionisation. It can be concluded that they are the anionic triplets. They are likely to be produced by excitation of the anionic ground-state molecules, and the value of pK_{a2}^* to be close to that of pK_{a2} . The non-observation of solvated electrons at pH 4 confirmed this hypothesis. The triplets arising from NAa, NAp and PAa were found to react with the starting compound. In the case of NAp it could be evidenced that the triplet gave a secondary transient species.

This secondary species can be assigned using the literature data. Indeed, the two bands 285/415 nm are reminiscent of those of 3-carboxypyridinyl radical, **1**, (see Fig. 4, dotted line).¹⁸ Subtracting from the global spectrum that of **1** yielded an absorption band in the region 300–360 nm resembling that reported for the OH-adduct radical (insert of Fig. 4).¹⁹ Taking for the extinction coefficients of **1** and OH-adduct radical the values reported in the literature ($7200 \text{ mol}^{-1} \text{ dm}^3 \text{ cm}^{-1}$ at 285 nm and $2000 \text{ mol}^{-1} \text{ dm}^3 \text{ cm}^{-1}$ at 325 nm, respectively) we computed from the products $\epsilon \times \phi$ measured in this work ($100 \text{ mol}^{-1} \text{ dm}^3 \text{ cm}^{-1}$ at 290 nm and $40 \text{ mol}^{-1} \text{ dm}^3 \text{ cm}^{-1}$ at 325 nm) that the radicals were both formed with $\phi = 0.02$. It shows that they are produced in the same pathway. By analogy to these results, we might expect to observe the 2-carboxypyridinyl radical, **2**, from acidic PA. Unfortunately, **2** exhibits an absorption spectrum ($\lambda_{\text{max}} = 305$ and 360 nm)²⁰ close to that of the end-of-pulse transient and its formation cannot be firmly proved. By subtracting the spectrum of **2** from the transient spectrum measured from acidic PA 2 μs after the pulse, we measured an absorption in the wavelength range 300–400 nm that may correspond to the OH-adduct radical by reference to the literature data²⁰ (see insert of Fig. 5).

In the case of PAa that shows the highest quantum yield of phototransformation, it was also possible to detect secondary species, one exhibiting a maximum at 290 nm that is likely to be **2** again, and another with a maximum at 400 nm that does not resemble any transient reported in the literature. The non-observation of **1** from NAa may be due to the overlapping of its absorption spectrum with that of the end-of-pulse species.

Proposed mechanism

pH < pK_{a1}. The product studies showed that the three isomers have the same behaviour all yielding hydroxylated derivatives with a chemical yield close to 40%. Based upon the results obtained by laser-flash photolysis with NA we can propose the mechanism given in Scheme 1. Using the fact that oxygen both quenches the triplet and decreases the quantum yield of photolysis, it can be deduced that the triplet state is involved in the reaction. Moreover, the detection of **1** and OH-adduct radical indicates that the reaction between the triplet and NA proceeds through an electron transfer. This reaction appears at a pH where molecules are protonated. However, an electron transfer between two protonated molecules seems very unlikely. As an alternative, we may

Table 2 Spectral characteristics and bimolecular rate constants of triplets

Triplet from	$\lambda_{\text{max}}/\text{nm}$	$k/\text{mol}^{-1} \text{ dm}^3 \text{ s}^{-1}$		
		substrate	O ₂	H ⁺
NAp	435	3.3×10^9	3.4×10^9	
NAa	285/375	1.3×10^9 (NAz) 4.8×10^8 (NAa)		4.6×10^9
PAp	306/350		2.4×10^9	
PAa	290/340	9.3×10^8 (PAz) 1.8×10^8 (PAa)		1.7×10^{10}
IAp	310/380			
IAa	290/375			

propose an electron transfer between the zwitterionic triplet and NAp. The formation of the zwitterionic triplet in a pH range where protonated ground state molecules are dominant is probably due to the deprotonation of the protonated triplet rather than by inter-system crossing of zwitterionic singlet, since no photoreactivity was observed in the pH range where zwitterions are the dominant forms. The weak photoreactivity of carboxypyridines at $pH < pK_{a1}$ can be explained by the small formation of zwitterionic triplet, by the difficulty of the electron transfer reaction or by a high probability of back electron transfer. The chemical yield of 40% for hydroxylated products and the formation of non-aromatic compounds visible on the NMR spectra suggest that an oxido-reduction occurs between pyridinyl radicals and OH-adduct, yielding hydroxylated derivatives and reduction products.

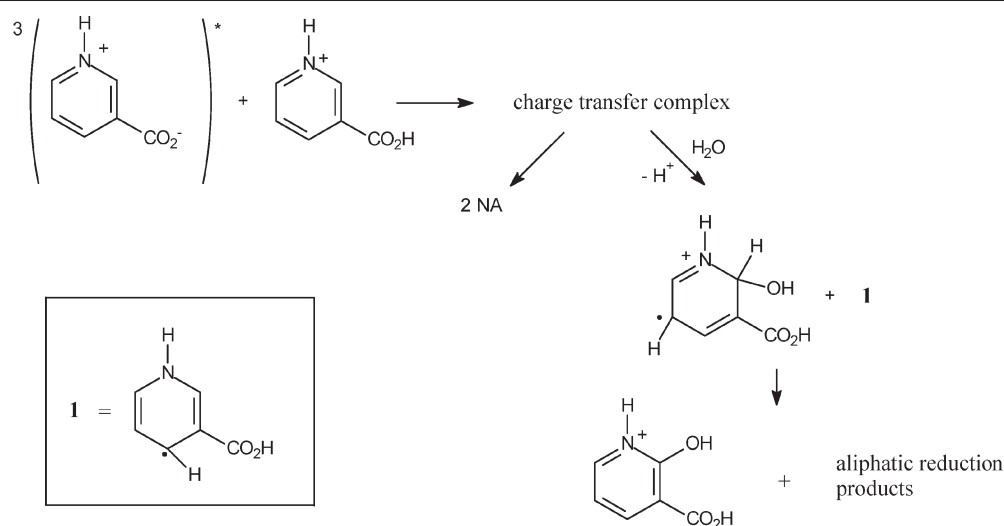
The long-lived species insensitive to oxygen produced from NA could not be attributed. It might be related to opening ring products described in the case of pyridine.⁷

2 < pH < 4. In this pH range that corresponds to $(pK_{a1} + pK_{a2})/2$ and in which compounds exist in the zwitterionic form, no transients were detected and no photoreactivity was observed. It is in accordance with a fast deactivation of zwitterionic singlet excited states.

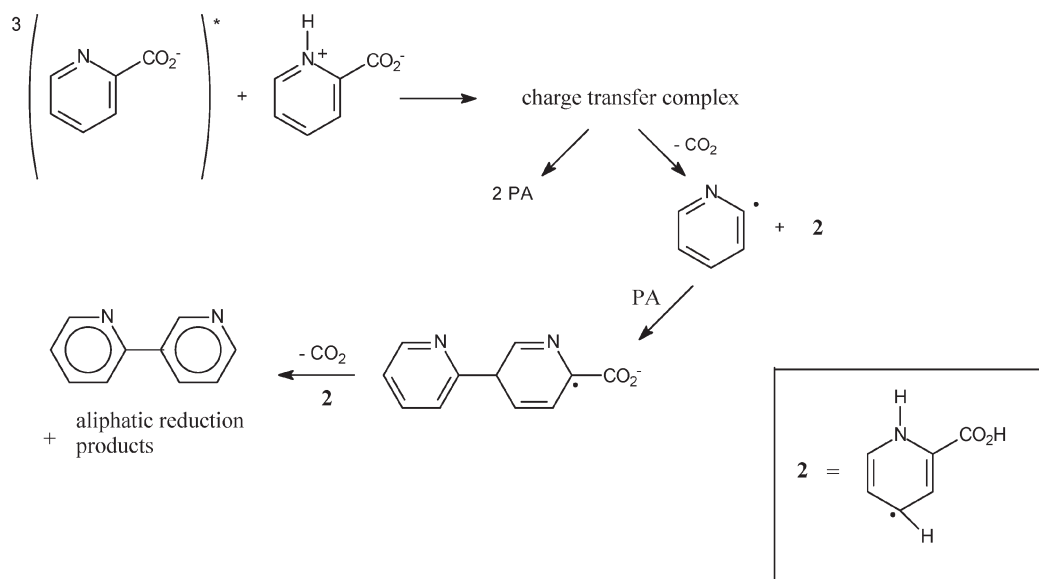
pH > 4. Under these pH conditions, IA is photostable while PA and NA photodimerize with different efficiencies. Results bring evidence that the triplet is involved in the photolysis again. First, oxygen both reduces the lifetime of the triplet and the quantum yield of the reaction. Second, the product $\epsilon \times \phi$ increases with increasing pH in the same pH range as the quantum yield of photolysis does. Third, IA, which is photostable, has a very short-lived triplet.

The detection of **2** from PA shows that again the initial reaction between triplet and ground state molecule is an electron transfer (Scheme 2). Molecular calculations showed that the C–CO₂⁻ bond order was lower in the charge transfer complex (0.77 and 0.48 for NA and PA respectively) than in the isolated triplet (1.05 and 0.98). Moreover, TOC measurements confirmed the CO₂ evolution. Since PA is more easily decarboxylated than NA, and also exhibits a higher quantum yield of photolysis, it seems that the decarboxylation process is the key step. It probably takes place at the level of the charge transfer complex competing with the return to ground-state molecules by reversible electron transfer. Pyridyl and anionic carboxypyridinyl radicals then escape the cage. The latter protonates (pK_a 5–6),^{18,20} while the pyridyl radical adds to a ground state molecule yielding an adduct. The long-lived species absorbing around 400 nm detected in PA solution might be this adduct. Lastly, a disproportionation reaction between this adduct and carboxypyridinyl radical occurs, yielding bipyridine and reduction photoproducts. In the case of PA, a second decarboxylation takes place, while in the case of NA carboxy-substituted bipyridines are formed. The structure of photoproducts shows that addition of the pyridyl radical occurs mainly in the *para* position, and probably in the *ortho* position too, with respect to the carboxy group. It yields only one photoproduct with PA because of the second decarboxylation, while it should yield three isomers with NA.

The stoichiometry of the reaction for PA is one bipyridine derivative produced for three PA molecules consumed. It is in very good accordance with the chemical yield found for bipyridine ($2 \times 28\%$) and with the quantity of CO₂ evolved ($0.9/8.9 \approx 2/18$). In the case of



Scheme 1

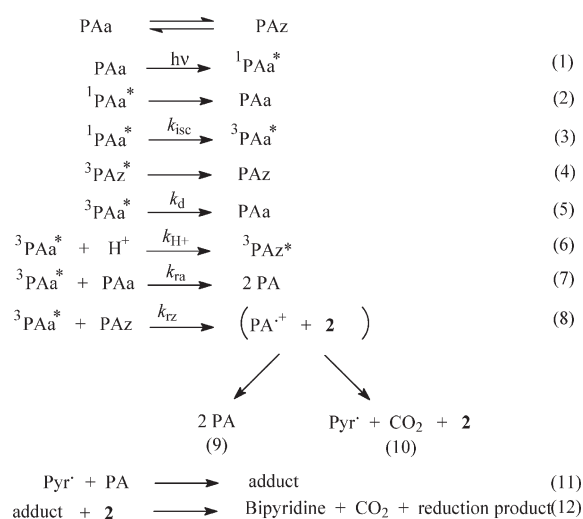


Scheme 2

NA, there should be a mole of CO_2 evolved for three NA molecules consumed (1/18). The experiments gave a result slightly higher, may be because the TOC measurement was performed at a high conversion extent (40 %).

On this basis, we propose the reaction mechanism described in scheme 2.

Assuming that the photoreactivity only arises from the anions, the mechanism in the case of PA can be written as shown in Scheme 3:



Scheme 3

where PAa and PAz are the anionic and zwitterionic forms respectively and Pyr^{\cdot} the pyridyl radical. The concentrations of PAa and PAz are given in eqn. 1 and the number of quanta absorbed by PAa in eqn. 2, where ε_z and ε_a are the molar extinction coefficients of PAz and PAa respectively, and A the absorbance of the solution at 254 nm.

$$[\text{PAa}] = \frac{[\text{PA}]}{1 + 10^{(\text{pK}_{\text{a}2} - \text{pH})}} \quad \text{and} \quad [\text{PAz}] = [\text{PA}] - [\text{PAa}] \quad (1)$$

$$I_a = \frac{I_o}{1 + \frac{\varepsilon_z}{\varepsilon_a} \cdot 10^{(\text{pK}_{\text{a}2} - \text{pH})}} \cdot (1 - 10^{-A}) \quad (2)$$

The rate of PA phototransformation is equal to:

$$-\frac{d[\text{PA}]}{dt} = r_1 + r_7 + r_8 + r_{11} - r_2 - r_4 - 2r_7 - 2r_9 \quad (3)$$

Applying the stationary state assumption to short-lived species, the rate becomes:

$$-\frac{d[\text{PA}]}{dt} = 3r_{10} = 3 \frac{k_9}{k_9 + k_{10}} r_8 = 3 \frac{k_9}{k_9 + k_{10}} \cdot k_{\text{rz}} [{}^3\text{PAa}^*][\text{PAz}] \quad (4)$$

and the stationary concentration of anionic triplet is given by:

$$[{}^3\text{PAa}^*] = \frac{I_a \phi_{\text{ISC}}}{k_d + k_{\text{H}^+}[\text{H}^+] + k_{\text{ra}}[\text{PAa}] + k_{\text{rz}}[\text{PAz}]} \quad (5)$$

where ϕ_{ISC} is the quantum yield of inter-system crossing. The quantum of PA photolysis that corresponds to:

$$\phi = -\frac{d[PA]}{dt} \cdot \frac{1}{I_o(1-10^{-A})} \quad (6)$$

is obtained by combining eqn. 4 and 5:

$$\phi = 3 \frac{k_9}{k_9 + k_{10}} \cdot \frac{\phi_{ISC}}{1 + \frac{\epsilon_z}{\epsilon_a} \cdot 10^{(pK_{a2} - pH)}} \cdot \frac{k_{rz}[PAz]}{k_d + k_{H^+}[H^+] + k_{ra}[PAa] + k_{rz}[PAz]} \quad (7)$$

Using eqn. 7 and the reaction rate constants measured by laser-flash photolysis experiments, we tried to fit the quantum yield dependences on pH and substrate concentration. First, we evaluated the bimolecular rate constants of reaction between triplet and the molecular ground state taking $k_{ra} = 1.8 \times 10^8 \text{ mol}^{-1} \text{ dm}^3 \text{ s}^{-1}$, and considering that the rate constant measured at pH = 5.1 was a linear combination of individual rate constants:

$$k_{observed} = k_{ra}[PAa] + k_{rz}[PAz]$$

We finally got $k_{rz} = 9.3 \times 10^8 \text{ mol}^{-1} \text{ dm}^3 \text{ s}^{-1}$. The plots $\phi = f(\text{pH})$ (Fig. 1) and $\phi = f([PA])$ (Fig. 2) could be well fitted taking for the product $\phi_{ISC} \cdot k_9 / (k_9 + k_{10})$, the value of 0.133. The same procedure was used for NA. From $k_{ra} = 4.9 \times 10^8 \text{ mol}^{-1} \text{ dm}^3 \text{ s}^{-1}$ we obtained $1.2 \times 10^9 \text{ mol}^{-1} \text{ dm}^3 \text{ s}^{-1}$ for k_{rz} . Again, curves of Figs. 1 and 2 were well fitted using 0.023 for the product $\phi_{ISC} \cdot k_9 / (k_9 + k_{10})$.

The product $\phi_{ISC} \cdot k_9 / (k_9 + k_{10})$ is about 6 fold higher for PA compared to NA while ϕ_{ISC} is about twofold lower if we refer to data of Fig. 10. It means that the ratio $k_9 / (k_9 + k_{10})$ is more than ten times higher for PA than for NA, in accordance with the easy decarboxylation process of the former.

In conclusion, this study clarifies the complex mechanism of phototransformation of carboxypyridines in aqueous medium. Triplet excited states were characterized and their involvement in the reaction established. It was shown that they react with the starting molecule by electron transfer to yield a reduced species (the pyridinyl radical) and an oxidized species. Depending on the protonation state of the nitrogen atom, this latter adds water or undergoes decarboxylation. These processes that prevent the back electron transfer from occurring are the key steps in the reaction. The position of the carboxy substituent with respect to the N atom is a crucial parameter. Indeed, the triplet of the *para* isomer that is deactivated very fast cannot react with the starting molecule rendering the *para* isomer photostable. This work stresses the importance of the protonation state of the nitrogen atom in the photochemistry of pyridine derivatives.

Experimental

Materials

Meta-carboxypyridine (nicotinic acid, NA) from Fluka, *ortho*-carboxypyridine (picolinic acid, PA), *para*-carboxypyridine (isonicotinic acid, IA), 6-hydroxynicotinic acid (6-OH-NA), 6-hydroxypicolinic acid (6-OH-PA) from Aldrich and 2-hydroxynicotinic acid (2-OH-NA), 2-hydroxypyridine and pyridine from Lancaster were used as received. Water was purified using a Millipore (Milli-Q) device.

Steady-state irradiations

For quantitative purpose, aqueous solutions of NA, PA or IA were irradiated in a quartz cuvette and in a parallel beam using a germicidal lamp (Philips TUV 6W) emitting at 253.7 nm under continuous stirring. Irradiations were also performed in a device equipped with six germicidal lamps in order to accumulate the photoproducts for their identification. Solutions were deoxygenated by argon bubbling or oxygenated by oxygen bubbling for 20 minutes prior to

irradiation. They were continuously stirred during the irradiation. Potassium ferrioxalate was used as a chemical actinometer. pH was generally adjusted using HCl or NaOH. For experiments conducted at pH values ranging from 5.5 to 6.0, it was necessary to buffer the solutions with phosphate buffers, because the pH slightly increased during the irradiations.

General techniques

UV-visible spectra were recorded on a Cary 3 (Varian) spectrophotometer. Proton and carbon NMR spectra were collected on both 300 and 500 Avance Bruker spectrometers, depending on the program used. The products were analyzed in solution in D₂O (4.8 ppm), CDCl₃ (7.28 and 77.3 ppm) or DMSO-d₆ (2.59 and 39.5 ppm) and the solvent was used as an internal reference. For ¹³C peak assignment, heteronuclear single quantum coherence (HSQC) was sometimes necessary to allow the attribution of all the resonances. HPLC-ESI-MS spectrometry analyses were performed by the Service Central d'analyse de CNRS, Solaize, France. A Hewlett-Packard model HP 1100-MSD was used to obtain the mass spectra. Products were separated on a column Waters X-Terra MS C₁₈-3.5 μm (2.1 mm × 150 mm). The temperature of the column was maintained at 50 °C. A mixture of HClO₄-acidified water (pH = 3.0)-acetonitrile (95%/5%, v/v) was used as eluent at a flow of 0.3 ml min⁻¹. Nitrogen was used as sheath gas at 13 l min⁻¹ and the spray voltage was 3 kV. Consumption of starting compounds and formation of photoproducts were monitored by analytical HPLC using a Waters apparatus equipped with a 996-photodiode array detector and a column Waters X Terra RP₁₈-5 μm (4.6 mm × 250 mm). The mobile phase was a mixture of H₃PO₄-acidified water (pH = 3.0)-acetonitrile (95/5%, v/v). The pHmeter was a 3310 Jenway. It was equipped with an Ag/AgCl glass combination electrode 9102 Orion.

Laser flash photolysis

Laser flash photolysis experiments were carried out on an Applied Photophysics LKS.60 apparatus equipped with a Nd : YAG laser Quanta-Ray GCR-130. The experimental procedure was described elsewhere.²¹ Samples were irradiated using the fourth harmonic ($\lambda = 266 \text{ nm}$, pulse duration 9 ns) in a 10 × 10 mm quartz cell. Solutions were deaerated by nitrogen bubbling directly in the cell and changed after each shot. Potassium peroxodisulfate was used as a chemical actinometer.

Photoproduct identification

2-OH-NA, 6-OH-NA and 6-OH-PA were identified by reference to commercially available products. The others compounds were obtained and identified as follows:

2-(3-Pyridyl)-pyridine-5-carboxylic acid. A deoxygenated solution of NA (30 ml, 10⁻³ mol dm⁻³, pH 5.0) was irradiated at 254 nm in the device equipped with six germicidal lamps for one hour to achieve a conversion extent of 50%. The reaction mixture was then evaporated to dryness in a rotary evaporator, under reduced pressure. The residue was used for ¹H-NMR analysis (¹H-¹H COSY sequence). (CDCl₃, δ ppm): 9.38 (d, 1H, *J* = 2.0 Hz), 9.25 (d, 1H, *J* = 2.0 Hz), 8.80 (dd, 1H, *J* = 5.0 and 2.0 Hz), 8.66 (dt, 1H, *J* = 7.9 and 2.0 Hz), 8.58 (dd, 1H, *J* = 8.0 and 2.0 Hz), 8.15 (d, 1H, *J* = 8.0 Hz), 7.77 (ddd, 1H, *J* = 7.9, 5.0 and 2.0 Hz). $\lambda_{max} = 246$ and 284 nm in H₂O at pH = 3.0. In order to determine the value of the molar extinction coefficient at 284 nm, we used NA as an internal reference. By using the ¹H-NMR data and integral measurement obtained for 2-(3-pyridyl)-pyridine-5-carboxylic acid and for NA in the mixture, and the HPLC area, we got $\epsilon = 5000 \pm 800 \text{ M}^{-1} \text{ cm}^{-1}$ at 284 nm for 2-(3-pyridyl)-pyridine-5-carboxylic acid.

The HPLC-ESI-MS analysis of a solution of NA (6 × 10⁻⁴ mol dm⁻³, pH 5.0) irradiated for 5 min in the absence of oxygen with six germicidal lamps gave a peak at *m/z* = 201 corresponding to [M + H]⁺ attributed to 2-(3-pyridyl)-pyridine-5-carboxylic acid and another at *m/z* = 245 with a fragment at *m/z* = 201 attributed to a dicarboxypyridine.

2-(3-Pyridyl)-pyridine. A deoxygenated solution of PA (30 ml, 6×10^{-4} mol dm $^{-3}$, pH 5.3) was irradiated at 254 nm in the device equipped with six germicidal lamps for 32 s to achieve a conversion extent of 50%. The reaction mixture was basified at pH 9.3 using NaOH. In these conditions, the only basic compounds could be selectively extracted using 60 ml of ethyl acetate, leaving the other products in the aqueous phase. The extract was dried and evaporated to dryness to give a nearly pure compound. $\lambda_{\max} = 227$ and 277 nm in H $_2$ O/CH $_3$ CN at pH = 3.0. For 1 H-NMR analysis, phase sensitive COSY-45 (homonuclear CORrelation SpectroscopY) sequence was necessary to improve the multiple double irradiations experiments

(Fig. 12). Note that this product was already prepared by Ishikura *et al.*²² *via* cross-coupling of pyridyl-borane derivative with the appropriate halogeno-pyridine, but no spectroscopic data were reported.

The HPLC-ESI-MS analyses were performed directly on a solution of PA (6×10^{-4} mol dm $^{-3}$, pH 5.34) irradiated for 35 s in the absence of oxygen with six germicidal lamps: $m/z = 157$ corresponding to $[M + H]^+$.

2-Hydroxyisonicotinic acid. Authentic sample of 2-hydroxy-IA was synthesized by stereoselective hydroxylation of the parent acid, *via* fluorination (gaseous F $_2$) in aqueous basic medium. After workup

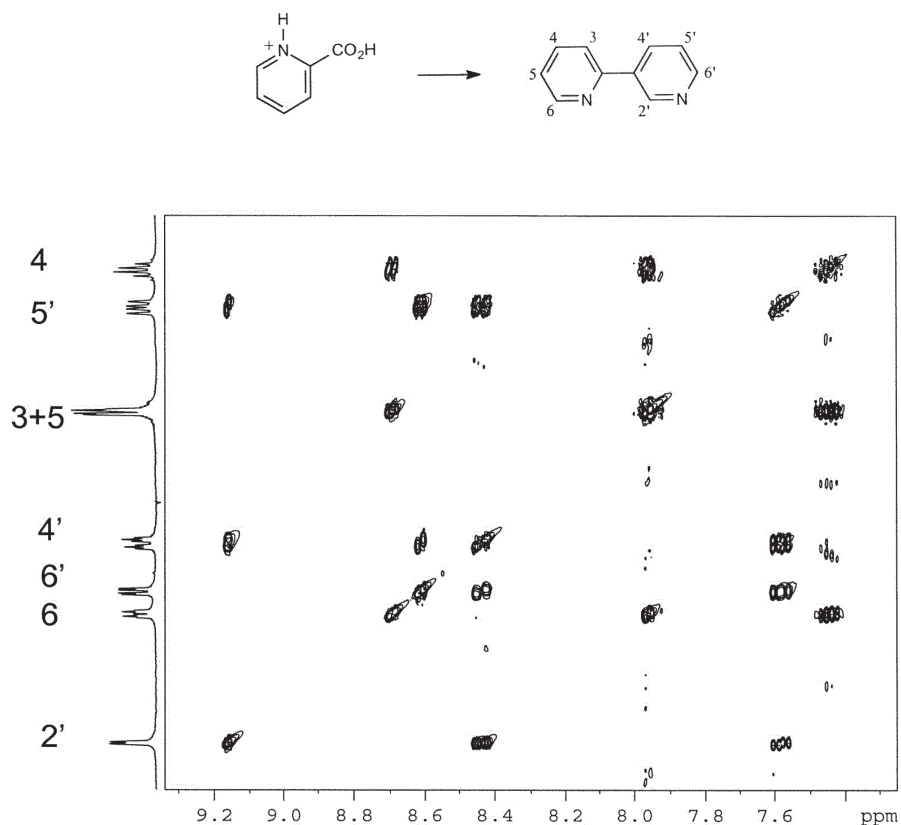


Fig. 12 1 H- 1 H Homonuclear correlation (COSY 45) spectrum of 2-(3-pyridyl)-pyridine.

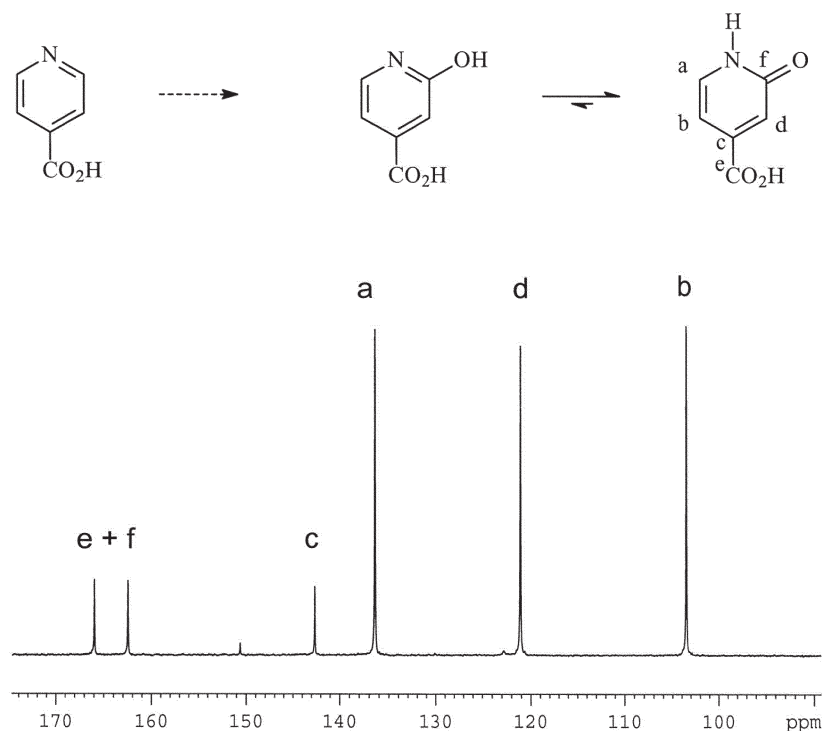


Fig. 13 13 C-NMR spectrum of 2-OH-IA (4-carboxy-2-pyridinone).

of these one-step procedure, as reported by Van Der Puy *et al.*,²³ the recrystallized product (AcOH/water 50/50; m.p. > 300 °C) was analysed by NMR spectroscopy. The proton spectrum (DMSO-d₆) shows three resonances of equivalent intensity at 7.5 ppm (d, $J = 7$ Hz, H⁶), 6.8 ppm (s, H³), and 6.5 ppm (d, $J = 7$ Hz, H⁵) besides a broad peak around 12.8 ppm (exchangeable with D₂O). The ¹³C spectrum (Fig. 13) clearly showed, here again, that the compound is in the pyridone form (two carbonyl resonances around 162.5 and 166 ppm).

Acknowledgements

We express our thanks to Professor D. Avignant (Université Blaise Pascal) for his help in the fluorine manipulations.

References

- 1 A. Lablache-Combier, Dérivés aromatiques azotés à six chaînons, in *Eléments de Photochimie Avancée*, P. Courtot, ed, Hermann, Paris, 1972, p. 293.
- 2 S. Caplain, J. P. Catteau and A. Lablache-Combier, *Chem. Commun.*, 1970, 1475.
- 3 S. Caplain, A. Castellano, J. P. Catteau and A. Lablache-Combier, *Tetrahedron*, 1971, **27**, 3541.
- 4 M. M. Alam, M. Fujitsuka, A. Watanabe and O. Ito, *J. Chem. Soc., Perkin Trans. 2*, 1998, 917.
- 5 R. Bernardi, T. Caronna, G. Poggi and B. M. Vittimberga, *J. Chem. Soc., Perkin Trans. 2*, 1990, 97.
- 6 T. Caronna, B. M. Vittimberga, M. E. Kornn and W. G. McGimpsey, *J. Photochem. Photobiol. A*, 1995, **90**, 137.
- 7 J. Jousset-Dubien and J. Houdard, *Tetrahedron Lett.*, 1967, **44**, 4389.
- 8 K. E. Wilzbach and D. J. Rausch, *J. Am. Chem. Soc.*, 1970, **92**, 2178.
- 9 L. Lindqvist, B. Czochralska, M. P. Fontaine-Aupart, W. Kawczynski, F. Tfibel and T. Douki, *Photochem. Photobiol. Sci.*, 2002, **1**, 600.
- 10 F. Takeuchi, T. Sugiyama, T. Fujimori, K. Seki, Y. Harada and A. Sugimori, *Bull. Chem. Soc. Jpn.*, 1974, **47**, 1245.
- 11 F. Rollet, C. Richard and J.-P. Aguer, *J. Photochem. Photobiol. A*, 2002, **153**, 33.
- 12 R. W. Green and H. K. Tong, *J. Am. Chem. Soc.*, 1956, **78**, 4896.
- 13 H. P. Stephenson and H. Sponer, *J. Am. Chem. Soc.*, 1957, **79**, 2050.
- 14 R. F. Evans, E. F. Herington and W. Kynaston, *Trans. Faraday Soc.*, 1953, **49**, 1284.
- 15 A. R. Katritzky and J. M. Lagowski, *Adv. Heterocycl. Chem.*, 1963, **1**, 339.
- 16 M. J. S. Dewar, J. Caoxian and Y. Jianguo, *Tetrahedron*, 1993, **49**, 5003.
- 17 Ampac7-0, 2000 Semichem, 7128 Summit, Shawnee, KS 66216.
- 18 P. Neta and L. K. Patterson, *J. Phys. Chem.*, 1974, **78**, 2211.
- 19 S. Solar, W. Solar, N. Getoff, J. Holcman and K. Sehested, *Radiat. Phys. Chem.*, 1988, **32**, 585.
- 20 G. R. Dey, D. B. Naik, K. Kishore and P. N. Moorthy, *J. Radioanal. Nucl. Chem.*, 1992, **163**, 391.
- 21 F. Bonnichon and C. Richard, *J. Photochem. Photobiol. A*, 1998, **119**, 25.
- 22 M. Ishikura, M. Kamada and M. Terashima, *Synthesis*, 1984, 936.
- 23 M. Van der Puy, D. Nalewajek and G. E. Wicks, *Tetrahedron Lett.*, 1988, **29**, 4389.